

**Does the fragments from decomposed ZIF-8 greatly affect some of the intramolecular proton-transfer of Thymine? A quantum chemical study**

Dejie Li, Ying Han, Huijuan Li, Ping Zhang, Qi Kang, Dazhong Shen\*

Corresponding author. Tel.: +86 0531 8618 0740; fax: +86 0531 8261 5258.

E-mail address: dzshen@sdnu.edu.cn (D. Z. Shen).

**Fig. S1** Irreversible change of the pore structure of ZIF-8 caused by water molecules.

**Fig. S2** The sketch map of mispairing of GT'.

**Fig. S3** The molecular structures of T and T'' investigated.

**Fig. S4** The optimized structures of M-T-nw-ts in the tautomeric processes.

**Fig. S5** The proton-transferred structures of M-T'-nw in the tautomeric processes.

**Fig. S6** Energy barriers change in the different tautomeric processes including T-nw→T''-nw, MT-nw→MT''-nw and M-T-nw→M-T''-nw.

**Table S1** The Optimized Geometrical Parameters of T and T' Including the Transition State T-ts

**Table S2** NPA Charge Distribution (au) on a Portion of the Critical Atoms in T-nw and MT-nw

**Table S3** Relative Energies of Proton-Transferred Complexes based on Initial Structures

**Table S4** NPA Charge Distribution (au) on the Portion of M-T-nw

**Table S5** Energy Barrier Comparison from B3LYP, CAM-B3LYP and MP2 Methods

**Table S6** Energy Barriers of T→T' Proton-transfer Processes Affected by Hydrated M-

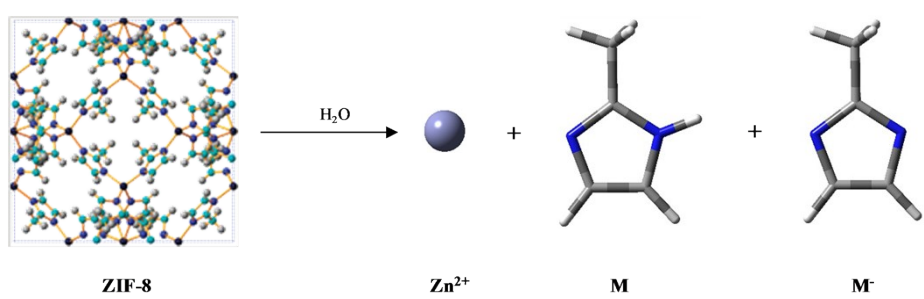


**Fig. S1** Irreversible change of the pore structure of ZIF-8 caused by water molecules.

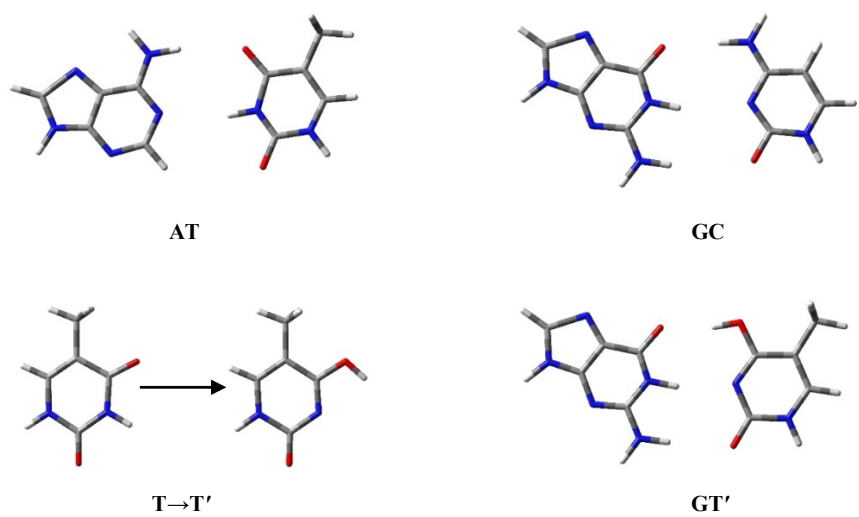


**Fig. S2** The sketch map of mispairing of GT'.

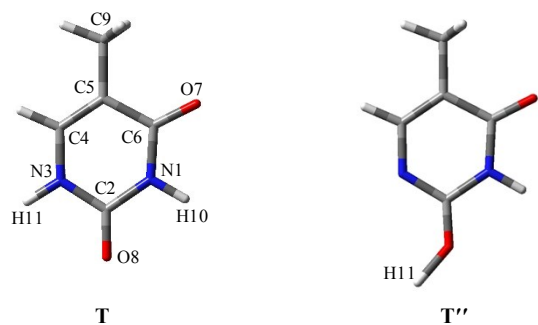


**Fig. S3** The molecular structures of **T** and **T''** investigated. O, C, N atoms are shown in red, gray and blue colors, respectively.

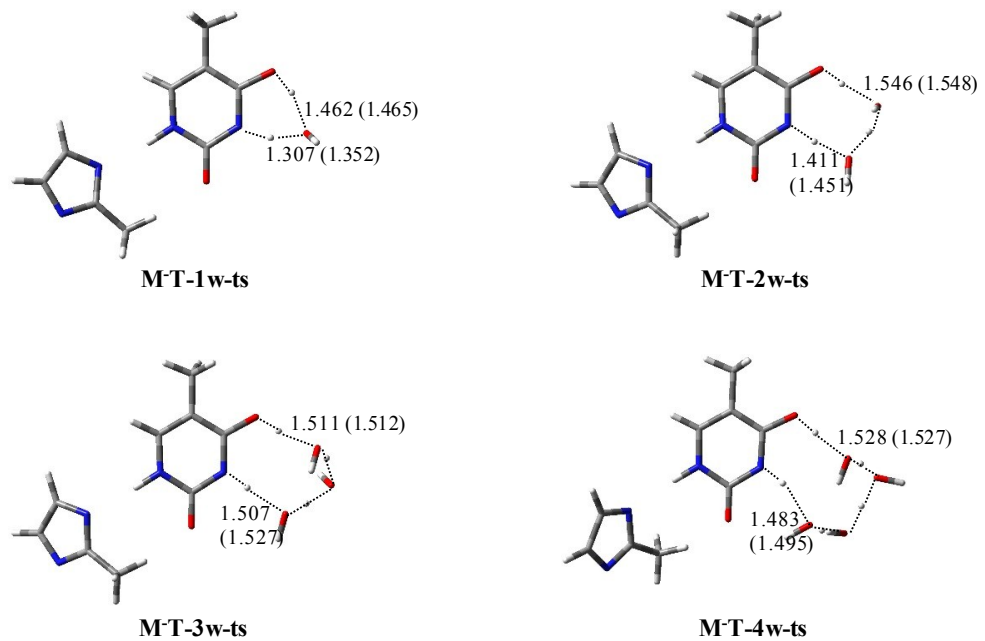


**Fig. S4** The optimized structures of M-T-nw-ts in the tautomeric processes. The route of proton-transfer are connected by dashed lines. Bond distances in angstrom ( $\text{\AA}$ ). Bond distances in parenthesis are obtained from MP2 method.

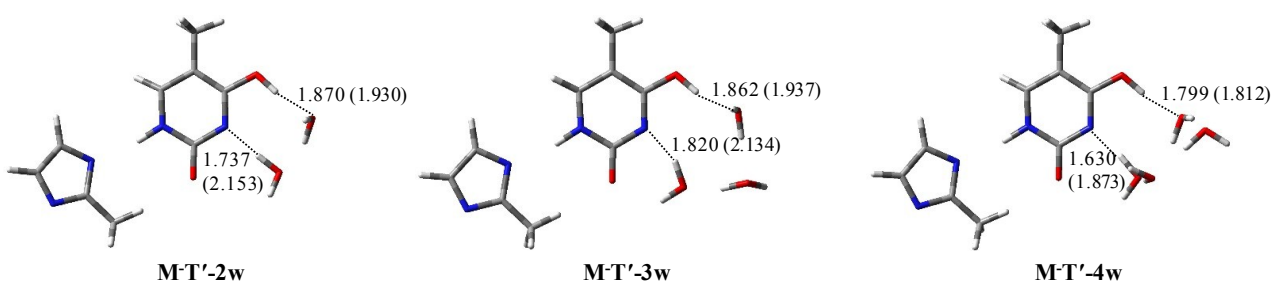


**Fig. S5** The proton-transferred structures of M-T'-nw in the tautomeric processes. The route of proton-transfer are connected by dashed lines. Bond distances in angstrom ( $\text{\AA}$ ). Bond distances in parenthesis are obtained from MP2 method.

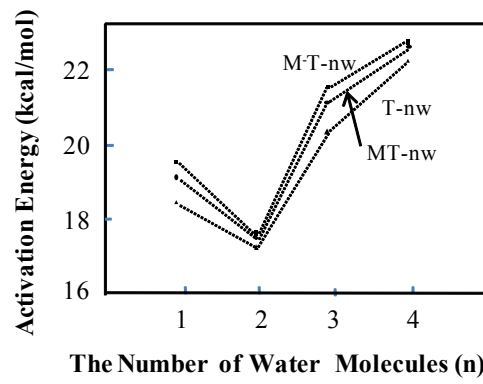


**Fig. S6** Energy barriers change in the different tautomeric processes including  $T\text{-nw} \rightarrow T''\text{-nw}$ ,  $MT\text{-nw} \rightarrow MT''\text{-nw}$  and  $M\text{-T}\text{-nw} \rightarrow M\text{-T''}\text{-nw}$ .

**Table S1** The Optimized Geometrical Parameters of T and T' Including the Transition State T-ts

bond	T	T-ts	T'	Ref. 35	Ref. 36
N1-C2	1.386	1.372	1.379	1.390	1.379
C2-N3	1.388	1.421	1.417	1.391	1.379
N3-C4	1.382	1.367	1.361	1.387	1.375
C4-C5	1.375	1.368	1.366	1.382	1.365
C5-C6	1.468	1.431	1.438	1.470	1.356
C6-N1	1.407	1.350	1.307	1.407	1.379
C6-O7	1.225	1.287	1.348	1.227	1.224
C2-O8	1.221	1.219	1.222	1.220	1.234
C5-C9	1.502	1.503	1.504	1.502	1.502

Bond length in Å.

**Table S2** NPA Charge Distribution (au) on a Portion of the Critical Atoms in T-nw and MT-nw (n=0-4)

n	T-nw / MT-nw <sup>a</sup>							
	O7	C6	N1	H10	O8	C2	N3	H11
0	-0.604(-0.619)	0.654(0.652)	-0.671(-0.668)	0.459(0.454)	-0.632(-0.660)	0.808(0.813)	-0.638(-0.647)	0.456(0.477)
1	-0.647(-0.661)	0.663(0.660)	-0.673(-0.669)	0.484(0.479)	-0.626(-0.653)	0.809(0.815)	-0.635(-0.643)	0.456(0.477)
2	-0.669(-0.683)	0.672(0.670)	-0.675(-0.672)	0.486(0.482)	-0.628(-0.654)	0.810(0.815)	-0.634(-0.642)	0.455(0.476)
3	-0.675(-0.686)	0.675(0.671)	-0.674(-0.671)	0.487(0.482)	-0.637(-0.666)	0.811(0.816)	-0.633(-0.640)	0.455(0.476)
4	-0.674(-0.665)	0.676(0.667)	-0.674(-0.675)	0.489(0.475)	-0.646(-0.665)	0.812(0.815)	-0.632(-0.643)	0.456(0.477)

<sup>a</sup> MT-nw data are listed in parenthesis.

**Table S3** Relative Energies of Proton-Transferred Complexes based on Initial Structures (0 kcal mol<sup>-1</sup>)

n	T'-nw	MT'-nw	M-T'-nw
0	11.0/11.2 <sup>a</sup>	12.0	15.1
1	10.5	10.9	12.0
2	8.9	9.2	10.5
3	8.8	9.1	9.6
4	8.4	9.9	10.8

<sup>a</sup> MP2/6-311++G\*\* basis set used in Ref 30. All computed values are zero-point energy corrected.

**Table S4** NPA Charge Distribution (au) on the Portion of M-T-nw (n=0-4)

n	M <sup>-</sup>	T	w
0	-0.570	-0.430	—
1	-0.510	-0.444	-0.046
2	-0.420	-0.530	-0.050
3	-0.399	-0.540	-0.061
4	-0.415	-0.528	-0.057

**Table S5** Energy Barrier Comparison from B3LYP, CAM-B3LYP and MP2 Methods

n	T-nw	MT-nw	M-T-nw
1	17.6 <sup>a</sup> / 21.3 <sup>b</sup> / 16.4 <sup>c</sup>	17.7 / 20.3 / 16.5	16.3 / 15.1 / 17.8
2	16.3 / 20.0 / 15.5	16.6 / 21.6 / 15.8	14.4 / 13.4 / 15.1
3	17.8 / 21.6 / 16.3	18.9 / 22.7 / 17.5	15.2 / 14.3 / 16.3
4	20.5 / 24.0 / 18.7	20.8 / 24.3 / 18.3	16.8 / 15.7 / 18.7

<sup>a</sup> obtained by B3LYP. <sup>b</sup> obtained by CAM-B3LYP. <sup>c</sup> obtained by MP2.

**Table S6** Energy Barriers of T→T' Proton-transfer Processes Affected by Hydrated M<sup>-</sup>

Proton-transfer structures	Energy barriers
(monohydrated M <sup>-</sup> )T-1w	16.7
(dihydrated M <sup>-</sup> )T-1w	16.5
(trihydrated M <sup>-</sup> )T-1w	16.4
(monohydrated M <sup>-</sup> )T-2w	15.8
(dihydrated M <sup>-</sup> )T-2w	15.6
(trihydrated M <sup>-</sup> )T-2w	15.5
(monohydrated M <sup>-</sup> )T-3w	17.3
(dihydrated M <sup>-</sup> )T-3w	16.8
(trihydrated M <sup>-</sup> )T-3w	16.6
(monohydrated M <sup>-</sup> )T-4w	20.1
(dihydrated M <sup>-</sup> )T-4w	19.5
(trihydrated M <sup>-</sup> )T-4w	19.3